



Science Arts & Métiers (SAM)

is an open access repository that collects the work of Arts et Métiers ParisTech researchers and makes it freely available over the web where possible.

This is an author-deposited version published in: <http://sam.ensam.eu>
Handle ID: <http://hdl.handle.net/10985/12059>

To cite this version :

Aldo ATTANASIO, Federico FAINI, José OUTEIRO - FEM Simulation of Tool Wear in Drilling -
Procedia CIRP - Vol. 58, p.440-444 - 2017

Any correspondence concerning this service should be sent to the repository

Administrator : archiveouverte@ensam.eu

16th CIRP Conference on Modelling of Machining Operations

FEM simulation of tool wear in drilling

A. Attanasio^{a*}, F. Faini^a, J.C.Outeiro^b

^aUniversity of Brescia, Via Branze 38, 25123 Brescia, Italy

^bLaBoMaP, Arts & Metiers Campus of Cluny, UBFC, HESAM, Rue Porte de Paris, 71250 Cluny, FRANCE

* Corresponding author. Tel.: +39-030-371-5584; fax: +39-030-370-2448. E-mail address: aldo.attanasio@unibs.it

Abstract

The objective of this study is to simulate tool wear in drilling of nickel-based alloys, in particular Inconel 718. When machining these kind of materials, the impact of the thermal and mechanical phenomena generated by tool wear on the surface integrity is of prime concern. For this reason, it is important to study the influence of tool wear on tool life, on final part quality and on cutting force and power consumption. Tool wear is caused by several phenomena (adhesion, abrasion, erosion, diffusion, corrosion, fracture etc.) depending on selected cutting parameters (cutting velocity, feed rate, etc.). In some cases these wear mechanisms can be described by analytical models which are function of physical quantities involved in process (temperature, pressure and sliding velocity along the cutting surface). Usually, commercial FEM software allows to implement these tool wear models but without tool geometry update. To overcome this limitation, a suitable subroutine considering tool geometry update was developed and implemented in SFTC DEFORM-3D FEA software to simulate tool wear in drilling of Inconel 718. A good agreement was obtained between the predicted and measured tool wear data.

© 2017 The Authors. Published by Elsevier B.V. This is an open access article under the CC BY-NC-ND license (<http://creativecommons.org/licenses/by-nc-nd/4.0/>).

Peer-review under responsibility of the scientific committee of The 16th CIRP Conference on Modelling of Machining Operations

Keywords: drilling, wear, modelling, Inconel 718

1. Introduction

Tool wear has a great influence not only on the tool life but also on the quality of the final product in terms of dimensional accuracy and surface integrity. These aspects are even more relevant in machining of difficult-to-cut materials such as nickel and titanium based alloys. These materials are used in applications that require high fatigue strength and good corrosion resistance, but those same characteristics become a problem during machining operations.

In the literature, it is possible to find several analytical/empirical equations that correlate tool flank wear length, VB, with the cutting conditions [1, 2]. However, time consuming and expensive experimental wear tests are often required to set-up such equations [3]. The numerical simulations of the machining operation can reduce the number of experimental tests. However, although tool wear models can be easily implemented or they are already available in

commercial FEA software, the tool geometry is not automatically updated in such softwares [4, 5].

This work is focused on the numerical simulation of tool wear in drilling of Inconel 718. Based on experimental wear data, the drill geometry is updated. An improved version of the algorithm for updating the tool geometry in turning [6, 7] was developed for drilling. This algorithm was implemented through a subroutine in the commercial FEA software DEFORM-3D version 11. Experimental data generated in a previous work [8] on drilling Inconel 718 under conventional metal working fluids (MWF) were used to validate the numerical simulation of drill wear.

2. Experimental set-up and parameters

Drilling tests were performed in a three-axes CNC milling machine DMG model DMU 65V, equipped with a designed experimental set-up for forces/torque and temperature

measurements. These tests were performed on nickel-based alloy work material, Inconel 718, solution-treated and age-hardened, having a hardness equal to 44 HRC (hereinafter referred to as IN718) using standard coated cemented carbide (TiAlN coating) twist drills. It is worth pointing out that these drills are designed to work with high pressure MWF, delivered to the cutting zone using the cooling channels in the drill (see Fig. 1). Drill geometry was inspected according to the ISO 3002-1/2 and DIN 1414-1/2 standards, as described by Astakhov [9], using both ZOLLER (models Genius3 and 3DCheck) and ALICONA (model InfiniteFocus) equipments. These equipments permitted to scan the tool geometry, which was used for tool inspection and to generate the drill CAD model for the numerical simulations (see Fig. 1). The tool inspection permitted to measure the following drill geometric parameters: drill diameter of 12.015 mm, back taper of 0.09° , helix angle of 30° , (four) margins width of 0.837 mm, point angle of 143.4° , drill run-out of 0.007 mm, chisel edge angle of 56.7° , chisel edge length of 0.397 mm, chisel edge centrality of 0.013 mm, web thickness of 0.173 mm, gash face angle of 64° , gash radius of 1.420 mm, normal rake angle varying from -10° to 32° , clearance angle varying from 10° to 18° and an average cutting edge radius of $55 \mu\text{m}$ [8]. The drilling tests were performed varying the cutting speed (v_c), and the feed (f). The values of these parameters were identified based on the toolmaker recommendation and after performing preliminary drilling tests under wide range of drilling conditions. Table 1 shows the cutting and MWF conditions used in the experimental drilling tests. The MWF was composed by 95 % of water and 5 % of a synthetic cutting fluid (supplied by TOTAL, commercial designation VULSOL 5000 S) at 20 bar pressure. During the drill tests axial force and drilling torque were measured using a piezoelectric dynamometer from KISTLER, models 9123C. Several drills were instrumented with thermocouples type K of 0.25 mm diameter.

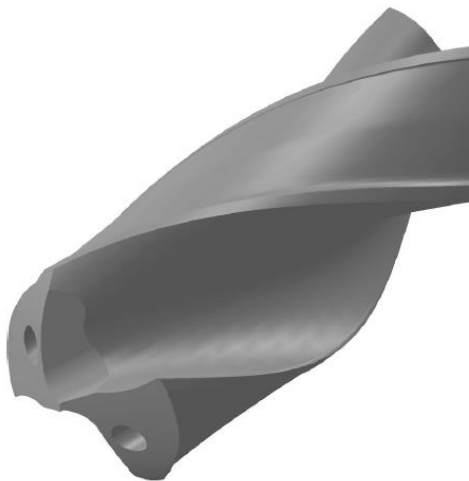


Fig. 1. Twist drill [8].

Table 1. Cutting parameters.

| Coolant conditions | | Cutting Parameters | | |
|--------------------|----------------|--------------------|--------------|------------|
| Fluid | Pressure [bar] | v_c [m/min] | f [mm/rev] | Hole depth |
| MWF | 20 | 10-30 | 0.08-0.11 | 10 |

In order to measure the temperatures as closest as possible of the cutting edge but at different locations, the thermocouples were placed at 1 mm from the cutting edges and at two locations: 0.74 mm (temperature T1) and 3.54 mm (temperature T2) from the drill margins (Fig. 2). During the temperature measurement tests the drill was kept static and fixed to the CNC milling machine table, while the workpiece was rotating and attached to the spindle using a designed fixation system, as shown in Fig 3. Special attention was paid in centering the tool in relation to spindle axis in order to minimize run-out errors.

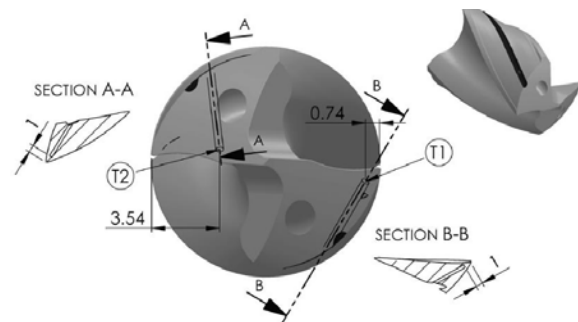


Fig. 2. Drill instrumentation with thermocouples type K for temperature measurements. T1 and T2 show the location of the thermocouples [8].



Fig. 3. Drill instrumentation with thermocouples type K for temperature measurements. T1 and T2 show the location of the thermocouples [8].

3. Numerical simulation

3.1. Model description

The workpiece (Fig. 4) has modelled as a plastic deformable with more than 45 000 tetrahedral elements with a minimum side length of about 0.1 mm. To model the thermo-viscoplastic behavior of the Inconel 718 alloy, the Johnson-Cook constitutive model [10], represented by equation (1), was employed.

$$\bar{\sigma} = \left(A + B \bar{\varepsilon}^n \right) \left[1 + C \ln \left(\frac{\dot{\bar{\varepsilon}}}{\dot{\bar{\varepsilon}}_0} \right) \right] \left[1 - \left(\frac{T - T_{room}}{T_m - T_{room}} \right)^m \right] \quad (1)$$

In this model, $\bar{\sigma}$ is the equivalent stress [MPa], $\bar{\varepsilon}$ is the equivalent plastic strain, $\dot{\bar{\varepsilon}}$ is the equivalent plastic strain rate [s^{-1}], $\dot{\bar{\varepsilon}}_0$ is the reference equivalent plastic strain ($0.001 s^{-1}$), T is the temperature [$^{\circ}C$], T_m is the melting temperature of the workpiece material ($1500^{\circ}C$) and T_{room} is the room temperature ($20^{\circ}C$). A , B , C , n , m are the J-C model coefficients, which for Inconel 718 are equal to 605 MPa, 1280 MPa, 0.0117, 0.139 and 3.98, respectively [8]. As far as the thermal properties of the Inconel 718 are concerned, they were taken from the Deform material database.

The tool (Fig. 5) was modelled as rigid and was meshed with more than 340 000 elements with a minimum side length of about 0.05 mm. Coated cemented carbide was selected as tool material and its thermal properties were taken from Deform material database.

It is important to note that the difference of mesh accuracy between workpiece and tool is justified by the research objective. Since the simulation want to study the tool wear development, the attention is focused on the tool. Following this idea, the workpiece was modelled with a small number of elements, in order to have a reduced computation times (hours instead of days).

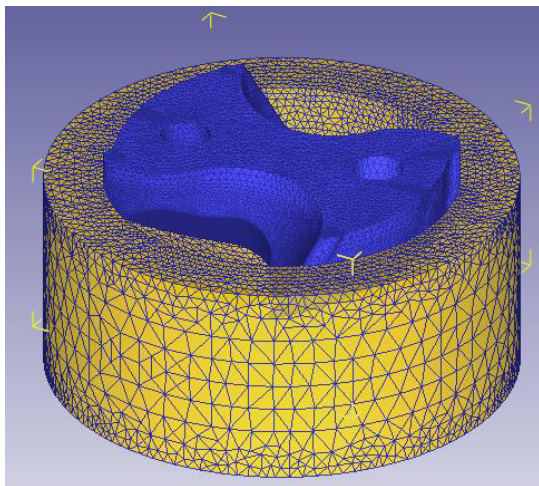


Fig. 4. The FEM model.

The tool-workpiece contact was implemented using the Zorev's model [11], expressed by equation (2).

$$\mu_{adh} = c_1 \times v_s + c_2 \quad (2)$$

The values of the coefficients of the Zorev's model c_1 and c_2 were found from tribological tests described in [12, 13] and they are equal to -0.004 and 0.340, respectively. This model was implemented in Deform environment through a suitable subroutine.

Regarding the coefficient of heat convection, it was modelled using the model proposed by Astakhov [9] and expressed by equation (3).

$$h_f = \frac{0.20}{b^{0.35} \times g^{0.33}} \cdot \frac{v_f^{0.65} \times k_f^{0.67} \times c_{p-f}^{0.33} \times \gamma_f^{0.33}}{v_f^{0.32}} \quad (3)$$

In this equation, b is the equivalent length [m], g is the acceleration due to gravity [m^2/s] and the remaining parameters are properties of the fluid. Equation (3) provided a value of $930 W/m^2 \text{ } ^{\circ}K$ for the MWF cooling. Based on the experimental measurements, an initial temperature of $20^{\circ}C$ has set to the workpiece and tool.

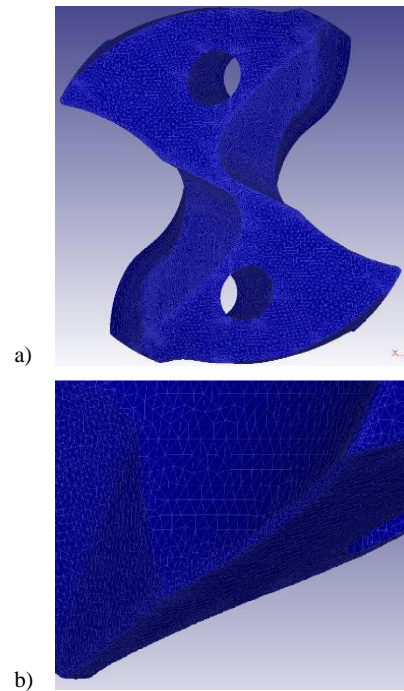


Fig. 5. (a) Tool mesh from $-z$ view; (b) Detail on the cutting edge.

3.2. Wear calculation and tool geometry update

Fig. 6 shows the flowchart of the adopted simulation strategy. The simulation of the tool flank wear is based on the application of a subroutine developed by the authors. The

subroutine was written in Fortran language, being this programming language supported by Deform. The subroutine should be applied after reaching the thermo-mechanical steady state. For this reason, the first step of the simulation strategy consists of running a standard incremental lagrangian simulation up to obtaining almost constant temperature and cutting force on both tool and workpiece (Step 1).

Before calculating the tool wear amount, the subroutine identifies the nodes of the tool that form the flank, the rake and the cutting edges (Step 2). These data are used to calculate in correspondence of each cutting edge node the local rake angle and the local clearance angle of the tool (Step 3).

At this point, the subroutine can estimate the local wear amount (Step 4) on the basis of:

- a given analytical wear rate (for instance the Takeyama and Murata's [1] or the Usui's model [2]) rather than on purely experimental data;
- the cutting edge node position.

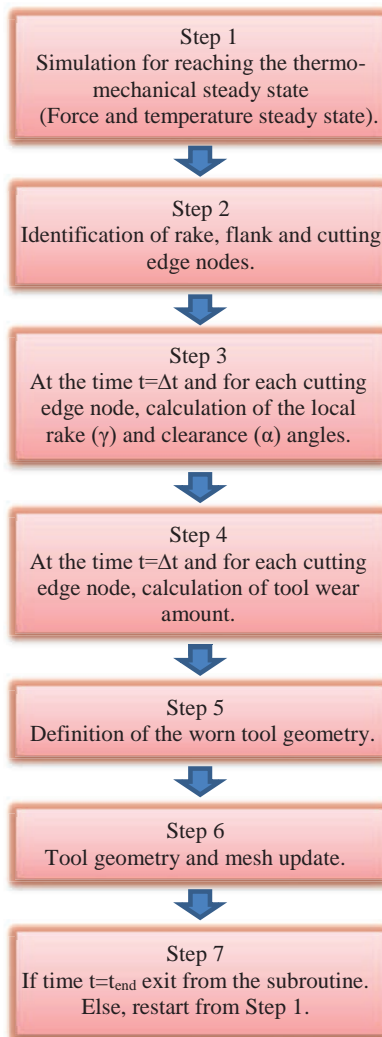


Fig. 6. Flowchart of the simulation strategy.

In fact, observing the experimental tool wear (Fig. 7), it is evident that the flank wear length VB increases from the drill center towards the margins. In particular, VB increases almost linearly from the drill center until the middle of the cutting edge (linear portion of the cutting edge), being constant along the curved cutting edge portion until the drill margins. This behavior can be attributed to the different cutting speed and to the tool geometry. As a consequence, the local tool wear amount is function of the node distance from the tool center.

Once estimated these parameters, the subroutine can define the nodes of the cutting edge that must be moved for a distance depending on the local value of VB, which depends on the current cutting time (Step 5). Next, the subroutine updates the tool mesh and geometry (Step 6).

This procedure is repeated up to reaching the final simulation time (t_{end} in Step 7).

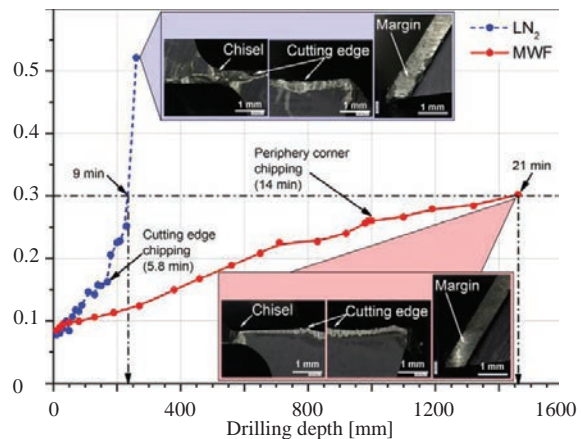


Fig. 7. Tool wear length (VB) in function of the drilling depth ($v_c = 24$ m/min, $f = 0.11$ mm/rev) [8].

3.3. Tool wear prediction

Fig. 8 shows the predicted distribution of tool flank wear after 6.5 minutes, 12 minutes and 21 minutes. As expected, the sub-routine predicts a growing flank tool wear as the cutting time increases. Some spikes due to the mesh size are noticeable on cutting edges and on the boundaries zones (i.e., the area where the flank wear finishes). For improving the quality of the FEM worn surface, smoothing algorithms will be introduced in the sub-routine. Fig. 9 shows a comparison between measured and predicted tool wear after 21 minutes. These figures show that the sub-routine is able to correctly reproduce the tool wear trend. In fact, the flank wear increases linearly from the drill center until the point at which starts the curved portion of the cutting edge. After this point, the wear is almost constant till the drill margins.

Fig. 10 shows the comparison between measured and predicted flank wear length VB. Low errors between predicted and measured data is noticed, ranging from -3.3% to +9.6% demonstrating that the developed simulation procedure can correctly simulate the tool wear in drilling operation.

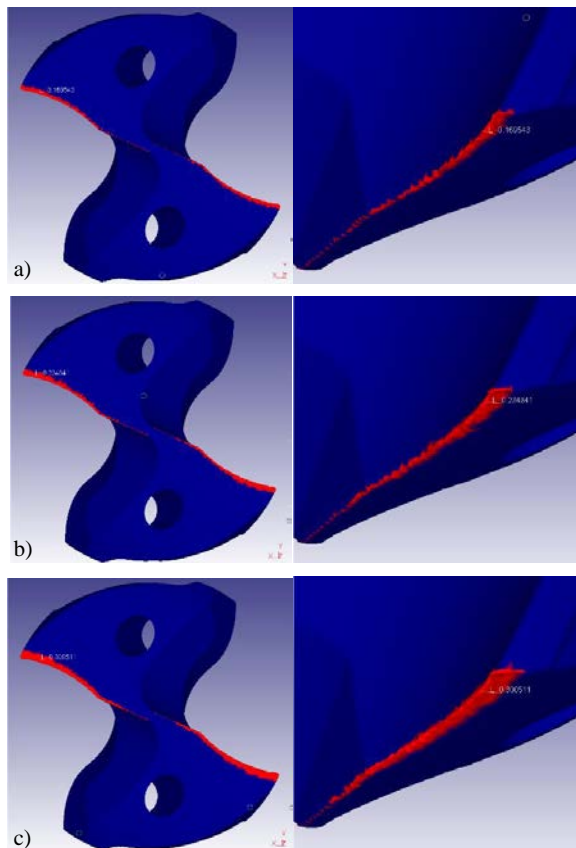


Fig. 8. Predicted flank wear distribution (frontal and cutting edge detail views) after 6.5 min (a), 12 min (b) and 21 min (c).

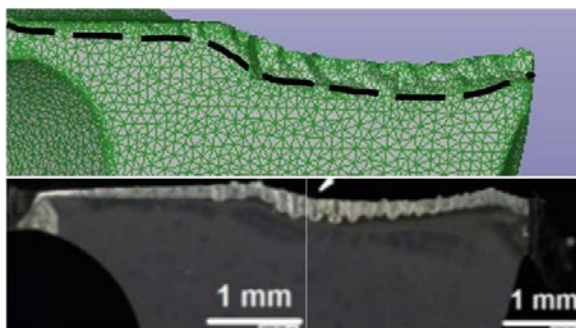


Fig. 9. Predicted and measured tool wear after 21 min.

4. Conclusions

This paper presents a research work on the development and application of a procedure to simulate the drill flank wear. A subroutine able to update the tool geometry based on empirical/experimental wear equations has been implemented in Deform-3D FEA software. For validating this procedure, the measured and predicted flank wear curves were compared. The

errors between both curves are low, demonstrating the accuracy of the developed procedure to capture the tool wear in drilling.

Further studies will be focused on implementing analytical wear models (e.g., Usui's or Takeyama-Murata's models) instead of empirical/experimental wear equations. So, it will be possible to simulate several cutting conditions, studying their effects on the process without the need of performing expensive and time consuming experimental tests.

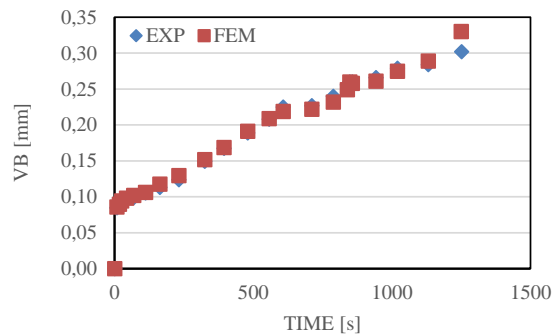


Fig. 10. Comparison between predicted and measured VB ($v_c = 24$ m/min, $f = 0.11$ mm/rev).

References

- [1] Takeyama H, Murata T, Trans. Basic Investigations on Tool Wear. Wear 85, 33-38 (1963).
- [2] Usui E, Shirakashi T, Kitagawa T, Trans. Cutting temperature and crater wear of carbide tools. Journal of Engineering for Industry 100, 236-243 (1978).
- [3] Poutord A, Rossi F, Poulachon G, M'Saoubi R, Abrivard G. Local approach of wear in drilling Ti6Al4V/CFRP for stack modelling. Procedia CIRP, 8, 316-321 (2013).
- [4] Yen YC, Söhner J, Weule H, Schmidt J, Altan T. Estimation of tool wear of carbide tool in orthogonal cutting using FEM simulation. Machining science and technology, 6(3), 467-486 (2002).
- [5] Xie LJ, Schmidt J, Schmidt C, Biesinger F. 2D FEM estimate of tool wear in turning operation. Wear, 258(10), 1479-1490 (2005).
- [6] Attanasio A, Ceretti E, Fiorentino A, Cappellini A, Giardini C. Investigation and FEM-based simulation of tool wear in turning operations with uncoated carbide tools. Wear 269 (5-6), 344-350 (2010).
- [7] Attanasio A, Umbrello D. Abrasive and diffusive tool wear FEM simulation. International Journal of Material Forming 2 (SUPPL. 1), 543-546 (2009).
- [8] Outeiro JC, Lenoir P, Bosselut A. Thermo-mechanical effects in drilling using metal working fluids and cryogenic cooling and their impact in tool performance. Production Engineering 9 (4), 551-562 (2015).
- [9] Astakhov VP. Tribology of metal cutting. Elsevier, London (2006).
- [10] Johnson GR, Cook WH. Fracture characteristics of three metals subjected to various strain, strain-rates, temperatures and pressure. Engineering Fracture Mechanics 21 (1), 31-48 (1985).
- [11] Zorev NN. Metal cutting mechanics. Pergamon Press, Oxford. (1966).
- [12] Courbon C., Pusavec F, Dumont F, Rech J, Kopac J. Influence of cryogenic lubrication on the tribological properties of Ti6Al4V and Inconel 718 alloys under extreme contact conditions. Lubrication Science 26, 315-326 (2014).
- [13] Zemzemi F, Rech J, Ben Salem W, Dogui A, Kapsa P. Identification of friction and heat partition model at the tool-chip/workpiece interfaces in dry cutting of an Inconel 718 alloy with CBN and coated carbide tools. Advances in Manufacturing Science and Technology 38, 5-22 (2014).